

Extended-state mobility and its relation to the tail-state distribution in *a*-Si:H

H. Michiel

Interuniversitair Micro-Elektronica Centrum v.z.w., Kapeldreef 75, B-3030 Heverlee (Leuven), Belgium

G. J. Adriaenssens

*Laboratorium voor Vaste Stof- en Hoge Druk-Fysica, Katholieke Universiteit Leuven,
Celestijnenlaan 200D, B-3030 Heverlee (Leuven), Belgium*

E. A. Davis

Department of Physics, University of Leicester, Leicester LE1 7RH, Leicestershire, England, United Kingdom
(Received 1 November 1985; revised manuscript received 3 March 1986)

The differing interpretations of drift-mobility data for electrons in *a*-Si:H have been examined. On the one hand, there are the analyses which involve the "thermalization approximation" (TA). One such analysis, based on the density-of-states profile deduced by Spear from field-effect data, leads to the unexpectedly high value of the extended-state mobility $\mu_{\text{ext}} = 500 \text{ cm}^2 \text{ V}^{-1} \text{ s}^{-1}$. Another analysis, which assumes an exponential distribution of tail states, results in the more commonly accepted value $\mu_{\text{ext}} = 13 \text{ cm}^2 \text{ V}^{-1} \text{ s}^{-1}$. In this work, we show that both models are inconsistent with experimental data when a more thorough examination is made of the field dependence and the activation energy of the drift mobility μ_d as predicted by those models. On the other hand, we examined Spear's analysis, which does not involve the TA. We show that a thorough analysis of multiple-trapping transport in a tail-state distribution as proposed by Spear leads to more dispersion than he experimentally observed. Our examination is based on a newly developed computational procedure, which analyzes multiple-trapping transport by discretizing the continuous distribution of localized states. Apart from the relevance with respect to electron transport in *a*-Si:H, this work shows how a relatively simple but accurate analysis of drift mobility and transient photocurrents can be performed with a much wider applicability than the analyses based on the TA.

I. INTRODUCTION

A curious state of affairs prevails concerning the interpretation of drift-mobility measurements in intrinsic hydrogenated amorphous silicon (*a*-Si:H). Whereas there is good agreement on the value of the electron drift mobility μ_d and its activation energy as measured by different groups on material prepared in several laboratories by the glow-discharge technique, strongly different conclusions concerning the extended-state mobility μ_{ext} and the tail-state distribution have been drawn from these observations. The electron drift mobility measured by Spear and his collaborators^{1,2} is about $1 \text{ cm}^2 \text{ V}^{-1} \text{ s}^{-1}$ at room temperature, with an activation energy of 0.13–0.14 eV in the temperature range 150–320 K (see Fig. 1, dashed line). In this temperature interval, transport is essentially non-dispersive, i.e., the narrow charge packet injected into the sample in a time-of-flight (TOF) experiment maintains its Gaussian shape during transit, as implied by the shape of the transient current and the independence of drift mobility on applied field. The measurements by Tiedje, Cebulka, Morel, and Abeles³ are in good agreement with Spear's at high temperatures; at lower temperatures, however, there is more dispersion than in Spear's data, as indicated by the different results obtained when the electric field is doubled (open *versus* solid circles in Fig. 1).

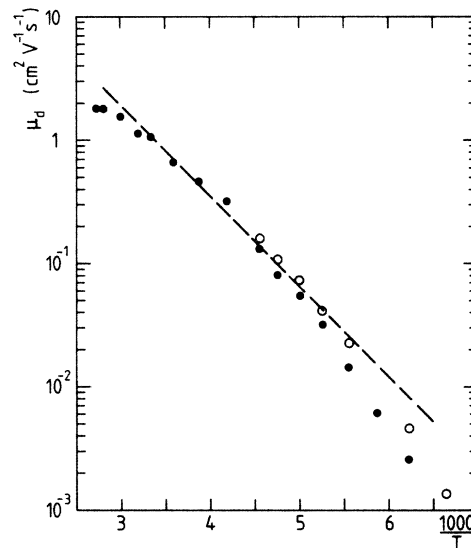


FIG. 1. Electron drift mobilities in undoped *a*-Si:H, measured in two laboratories. The dashed curve represents the results obtained by Spear *et al.* (Ref. 1) for electric fields varying by a factor of 10. The solid (open) circles are measurements by Tiedje *et al.*³ on a 3.9- μm thick sample at a field of 10^4 (2×10^4) V cm^{-1} .

The deduction of a correct value for the extended-state mobility μ_{ext} from the measured drift mobility μ_d is of great importance, since μ_{ext} is directly related to the preexponential factor in the conductivity, and thus carries considerable interest in the study of transport in amorphous semiconductors.⁴ It is also of importance for the performance of field-effect transistors (FET's) based on *a*-Si. It is therefore rather disturbing that some authors¹⁻³ find $\mu_{\text{ext}} \approx 10 \text{ cm}^2 \text{ V}^{-1} \text{ s}^{-1}$, whereas Silver, Snow, and Adler⁵ estimate $\mu_{\text{ext}} \geq 500 \text{ cm}^2 \text{ V}^{-1} \text{ s}^{-1}$, an almost crystalline value, *on the basis of the same experimental results*. Unexpected as Silver's assertion may be, it nevertheless deserves careful examination, for a crystalline value for μ_{ext} would have drastic consequences for the theory of the mobility edge⁴ and would open new perspectives on device fabrication. Such a high value for μ_{ext} is also by itself surprising because it contradicts accepted notions about noncrystalline semiconductors.⁶

The arguments advanced by Silver and co-workers to support this unexpectedly high mobility are briefly summarized. On the basis of highly similar transient responses in amorphous and crystalline silicon *p-i-n* photodiodes it was suggested that the two types of material have comparable extended-state mobilities. At the same time it was shown that, in conjunction with an exponential distribution of traps extending 0.5 eV below the band edge, a value of $\mu_{\text{ext}} = 800 \text{ cm}^2 \text{ V}^{-1} \text{ s}^{-1}$ can be used to describe the transient space-charge-limited currents in a $n^+ - i - n^+$ *a*-Si:H device.⁷ Such high mobilities are consistent with a lack of geminate recombination in *a*-Si:H,⁸ and they would also explain the nonobservance of a predicted initial rise in band-tail luminescence.⁹ Finally, Silver *et al.* also claim that a realistic analysis of published drift-mobility data will lead to extended-state mobility values of about $500 \text{ cm}^2 \text{ V}^{-1} \text{ s}^{-1}$.^{5,10} A negative result in reverse-recovery experiments was first seen as further support for a high value of the mobility,^{11,12} but other investigators^{13,14} showed that such conclusion was unwarranted. It is the analysis of TOF drift-mobility measurements that will concern us in this paper. Silver *et al.* base their analysis on a multiple-trapping (MT) transport model in a density-of-states distribution similar to the one advanced by Spear on the basis of field-effect measurements in *a*-Si:H.¹ Silver's analysis further uses the thermalization depth concept, an approximation introduced by Tiedje and Rose¹⁵ and Orenstein and Kastner;¹⁶ the thermalization approximation will be indicated by TA in what follows.

Let us now consider the analyses which lead to the more common low mobilities. Spear's interpretation is straightforward.^{1,2} The activation energy of the drift mobility, ΔE , is interpreted as the energy depth below the conduction band of a narrow range of states around an energy E_a which effectively control transport during transit. From the nondispersive character of the transient photocurrent in his experiments, it is deduced that the excess carriers are in quasithermal equilibrium with these states. It then follows that the proportionality factor between μ_{ext} and μ_d is $(n_c + n_t)/n_c$, where n_c is the density of free excess carriers and n_t the density of trapped excess charge. Quasithermal equilibrium then leads to

$$\mu_d \approx \mu_{\text{ext}} \left[1 + \frac{g(E_a)}{g(E_c)} \exp \left(\frac{\Delta E}{kT} \right) \right]^{-1}, \quad (1)$$

where $g(E_c)$ is the density of states at the conduction-band mobility edge, and $g(E_a)$ the corresponding quantity for the transport-controlling states. If $E_a - E_c = \Delta E = 0.13 \text{ eV}$ and $g(E_a)/g(E_c) = 10^{-1}$ as suggested by the field-effect data, one obtains $\mu_{\text{ext}} = 17 \text{ cm}^2 \text{ V}^{-1} \text{ s}^{-1}$. (Note that the energy is measured from the conduction-band mobility edge at $E_c = 0$ toward midgap, as in Fig. 2.)

Almost the same value ($\mu_{\text{ext}} = 13 \text{ cm}^2 \text{ V}^{-1} \text{ s}^{-1}$) was deduced by Tiedje *et al.*³ on the basis of a more detailed argumentation making use of the TA method. However, the analysis of Tiedje *et al.* can be challenged on a number of points. The good agreement with Spear's value of mobility would then be rather accidental. To be more precise, the TA has been developed for the analysis of anomalously dispersive transient currents, whereas electron transport in glow-discharge *a*-Si:H is not strongly dispersive in the temperature range of interest here. Furthermore, the analysis of Tiedje *et al.* assumes that the localized tail states exponentially decrease in density *from*

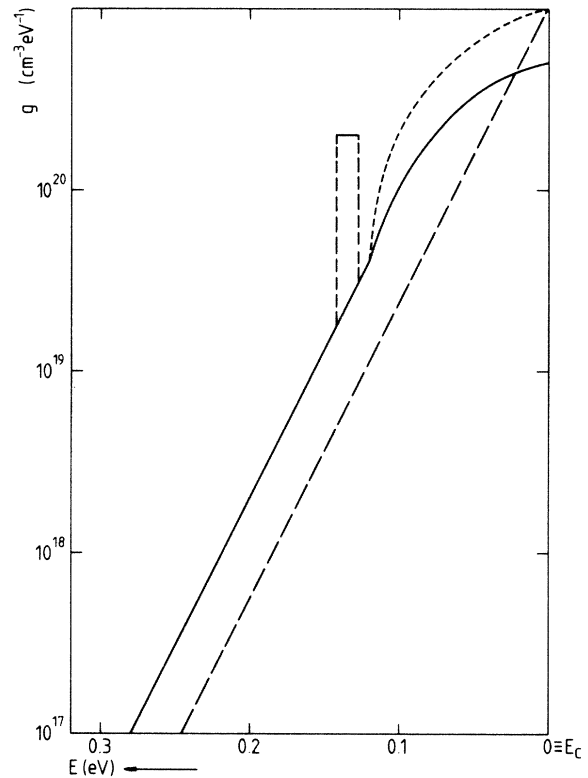


FIG. 2. Density-of-state models used in the simulations. The dashed curve is an exponential tail with a characteristic temperature $T_c = 310 \text{ K}$. The solid curve consists of a linear tail from E_c to $E_c + 0.12 \text{ eV}$, and is followed by an exponential distribution with $T_c = 310 \text{ K}$. An alternative model to the solid curve has a steeper linear part, shown as a dotted line. The rectangle is a feature added by us in order to study the influence of a peak in the tail-state distribution. All distributions have a cutoff at 0.30 eV .

the mobility edge downwards (Fig. 2, dashed line), which is quite different from the distribution advanced by Spear. We finally note that the TA itself is an approximation whose limitations have not been thoroughly examined (see, however, Refs. 17 and 18).

The situation concerning the interpretation of drift-mobility data in *a*-Si:H can thus be summarized as follows. Interpreting μ_d data on an exponentially decaying density-of-states (DOS) model and using the TA, Tiedje *et al.*³ obtain $\mu_{\text{ext}} \approx 10 \text{ cm}^2 \text{ V}^{-1} \text{ s}^{-1}$. Silver *et al.*,⁵ on the other hand, also using the TA and assuming a DOS of the type deduced by Spear from field-effect measurements obtain $\mu_{\text{ext}} \approx 500 \text{ cm}^2 \text{ V}^{-1} \text{ s}^{-1}$. Finally, Spear^{1,2} finds $\mu_{\text{ext}} \approx 10 \text{ cm}^2 \text{ V}^{-1} \text{ s}^{-1}$ on assuming that transport is controlled by states some 0.13 eV below the mobility edge. However, this last analysis does not show convincingly why the states at 0.13 eV predominate and cannot be applied to experimental results as Tiedje's, which show a certain field dependence (dispersion) of the drift mobility.

It is the purpose of this article to examine the various models that have been used in obtaining the contradictory results summarized above and to see how well they can account for the observed field and temperature dependences. To this end, we make use of a new computational technique which permits us to calculate the transient current, the trap occupations, the transit time, and the mobility for multiple-trapping transport in an arbitrary distribution of traps. This technique does not involve the TA. Although it is very accurate, it requires only simple algebra in its mathematical tool box. This computational approach is presented in Sec. II. In Sec. III, we examine the TA and its application to an exponentially decreasing DOS. This is the model proposed by Tiedje *et al.*³ to explain drift-mobility data in *a*-Si:H. It will be shown that an exponential DOS is unable to explain the essentially nondispersive transient photocurrent and the well-defined activation energy ΔE of μ_d . We then use Spear's DOS for *a*-Si:H and show that an interpretation of Spear's μ_d data within this model would lead to an extended-state mobility of about $50 \text{ cm}^2 \text{ V}^{-1} \text{ s}^{-1}$, which is considerably larger than $10 \text{ cm}^2 \text{ V}^{-1} \text{ s}^{-1}$, but still lower than $500 \text{ cm}^2 \text{ V}^{-1} \text{ s}^{-1}$. However, the agreement with experimental data is rather poor, in that the drift-mobility activation energy would be larger than observed, and would depend on the temperature as well as on the electric field or the sample thickness. In Sec. V, we investigate the possibility that additional features in the proposed DOS could give better agreement with the μ_d data. One such feature has been suggested by Marshall^{2,19} and consists of a sudden drop in the capture cross sections for states below 0.13 eV. Another possibility which we investigate is a peak in the DOS around that energy.

The main conclusions of this paper, summarized in Sec. VI, are the inappropriateness of either the exponential tail of localized states as proposed by Tiedje or the DOS proposed by Spear to explain the various aspects of available drift-mobility data. Although our simulations suggest an extended-state mobility $\mu_{\text{ext}} \approx 50 \text{ cm}^2 \text{ V}^{-1} \text{ s}^{-1}$ which is somewhat higher than deduced before, we see no way to reconcile $\mu_{\text{ext}} = 500 \text{ cm}^2 \text{ V}^{-1} \text{ s}^{-1}$ with experimental data.

Finally, after having performed the calculations for

these particular models, we are able to better evaluate the applicability of approximate methods as the TA. It was found that the results of the TA are in good agreement with our more precise method for the DOS models with continuously decreasing densities as considered here. However, serious discrepancies would result if the TA were applied to more general DOS models, for which case we show that a correct expression for the drift mobility is the critical issue.

II. COMPUTATIONAL PROCEDURE

We assume that transport is in extended states above the conduction-band mobility edge at energy E_c , and that the contribution of the holes to the current can be neglected (because of a large difference in the drift mobility, as is the case for *a*-Si:H or because of the geometry of the problem, as in a TOF experiment with negative top surface). Free excess electrons at E_c are stochastically trapped into the localized states at energies E below E_c , with the trapping probability $d\omega$ per second into states within the infinitesimal energy interval dE given by

$$d\omega(E) = g(E)dE \sigma(E)\bar{v}, \quad (2)$$

where $g(E)$ is the density²⁰ and $\sigma(E)$ the capture cross section of the traps, and where \bar{v} is the average velocity of electrons at the mobility edge.²¹ Trapped electrons will be released to the conduction band with a probability per second equal to

$$r(E) = \nu(E)\exp(-E/kT), \quad (3)$$

where $\nu(E)$ is an attempt-to-escape frequency for states at an energy E . We explicitly exclude transitions between the trapping states (hopping), not only to obtain a tractable model, but also since Halpern²² has shown that hopping makes a negligible contribution to the transport for the temperature range of interest here.

Using (2), (3), and a model $g(E)$, one can write down the rate equations for trapping and release in the form of integro-differential equations. An analysis of MT transport along these lines has been given by Rudenko and Arkhipov^{23,24} but, due to its mathematical intricacy, their procedure is difficult to apply to arbitrary DOS models. In an earlier paper²⁵ we have shown how this difficulty can be circumvented. We replace a continuous distribution of localized states by a series of discrete levels at equal energy intervals δE . In this way, the integro-differential equations become first-order differential equations with constant coefficients, which can be solved by simple matrix methods. The time dependence of n_c , the excess free-carrier density, or n_i , the excess occupation of any of the discrete levels can be obtained. These solutions are in the form of a sum of exponentials plus a constant.

In what follows, we will assume that the capture cross sections and attempt-to-escape frequencies are constant over the localized levels of interest. This is not a necessary ingredient of our procedure, but too little is known of a possible variation of these quantities in *a*-Si:H for its incorporation in the calculations to be meaningful (see, however, Sec. V). In the discretized approach, the rate equations are the following:

$$\frac{dn_c}{dt} = \sum_{i=1}^M r_i n_i(t) - n_c(t)W, \quad (4)$$

$$\frac{dn_i}{dt} = n_c(t)\omega_i - n_i(t)r_i \quad (i = 1, 2, \dots, M). \quad (5)$$

Equation (4) is the rate equation for the conduction band with n_c the excess density of free carriers; the M equations (5) describe the excess occupation n_i of the M discrete levels. The other parameters are given by

$$r_i = v \exp(-E_i/kT) = \tau_{rel,i}^{-1}, \quad (6)$$

where $\tau_{rel,i}$ represents the mean release time for an electron in the i th trap species, and

$$\omega_i = N_i \sigma \bar{v} = \tau_{trap,i}^{-1} \quad (7)$$

with

$$N_i = g(E_i) \delta E \quad (8)$$

being the integrated density²⁶ (in cm^{-3}). In (4),

$$W = \sum_{i=1}^M \omega_i \quad (9)$$

and $W^{-1} = \tau_{trap}$ represents the average trapping time. The system of equations (4) and (5) must be completed by an appropriate initial condition. For a TOF experiment, this is the following:

$$n_c(0) = n_0; \quad n_i(0) = 0 \quad (i = 1, 2, \dots, M), \quad (10)$$

where n_0 is the density of excited carriers.

We also note that the trapping and release probabilities are not independent quantities. They are related through the detailed-balance condition which expresses the equality of the number of upward and the number of downward transitions between any two energy levels in thermal equilibrium. For transitions between a trapping level and the conduction band, which is represented by an effective density-of-states N_c given by

$$N_c = g(E_c) kT, \quad (11)$$

detailed-balance results in the relation

$$v/\sigma \bar{v} = N_c. \quad (12)$$

The detailed-balance relation (12) will prove very useful in what follows. Although one should always be aware that strictly it defines a relation between equilibrium values of the parameters and that the application of an electric field could distort relation (12), we will assume its validity under the conditions normally met in a TOF experiment.

The approach to MT transport for an arbitrary DOS sketched above is suited for the analysis of anomalously dispersive as well as for conventional Gaussian transport. In Ref. 25 we not only demonstrated the accuracy of the discretization procedure when analyzing continuous distributions, but were able to solve the "spectroscopic" problem of MT transport (i.e., to find a DOS which results in a given transient photocurrent) with the same elementary matrix methods. Although an analysis of MT transport in terms of discrete levels has been presented earlier by other authors,²⁷ the Laplace-transform tech-

nique, which forms the backbone of those analytical treatments, makes the study of MT transport in an arbitrary DOS rather difficult. We therefore believe that our matrix approach has considerable advantages, as it also makes the spectroscopic analysis of experimental data feasible. Independently, Maschke, Merk, and Czaja²⁸ have used the same discretization procedure for the interpretation of photoluminescence spectra in α -Si:H.

The solution of the trapping equations gives the occupations of the transport states and the traps at any time for a sample of infinite length (no carrier loss at the back electrode). However, for the interpretation of TOF experiments and drift-mobility data, it will be necessary to consider samples of finite length and to relate the transit time t_{tr} to the transport parameters, the sample thickness, and the applied electric field. This is clearly not possible with the rate equations (4) and (5), because the position of the carriers does not appear in these expressions. This is a consequence of our implicit assumption of homogeneous material, of our neglect of trap occupation statistics on the trapping probability (no saturation of traps), of not taking into account diffusion, and of the exclusion of hopping between the traps. (Hopping, especially when it also involves "R hopping" between isoenergetic states, is critically dependent on the spatial distribution of the states, and is clearly beyond the scope of our rate-equation approach.) Fortunately, a formula suitable to our formalism, and which gives a good approximation to the transit time t_{tr} for the case of MT transport (whether dispersive or not) has been introduced in Ing, Neyhart, and Schmidlin²⁹ and was used subsequently^{27,30} by several authors. This formula is the following:

$$t_{tr} \simeq t_0 + \sum_i' M_i v^{-1} \exp(E_i/kT). \quad (13)$$

Here, t_0 represents the free transit time of carriers which do not interact with the traps

$$t_0 = L/\mu_{ext} F, \quad (14)$$

with L the sample thickness and F the electric field strength; M_i is the expected number of times a carrier is captured in the i th kind of trap during the time t_0 :

$$M_i = N_i \sigma \bar{v} t_0 = \omega_i t_0 \quad (15)$$

with N_i the density of the i th discrete trap species. The prime on the summation sign is used to indicate that the summation in (13) is to be performed over only those levels for which $M_i \geq 2$. Equation (13) is easily understood, as $v^{-1} \exp(E_i/kT)$ is the mean time a trapped carrier is immobilized in the i th trap species [see Eq. (6)]. It is also very natural to include only those levels for which $M_i \geq 2$, because $M_i < 2$ represents "deep trapping" on the time scale t_{tr} .

Another aspect of Eq. (13) becomes more transparent if the detailed-balance result (12) is applicable. Substituting (12) and (15) into (13) gives

$$t_{tr} \simeq t_0 \left[1 + \sum_i' (N_i/N_c) \exp(E_i/kT) \right]. \quad (16)$$

The self-evident relation between the free and the trap-controlled transit times, on the one hand, and the drift

and extended-state mobilities on the other,

$$t_0/t_{tr} = \mu_d/\mu_{ext}, \quad (17)$$

gives then the following expression for the drift mobility:

$$\mu_d = \mu_{ext} \left[1 + \sum_i' (N_i/N_c) \exp(E_i/kT) \right]^{-1}. \quad (18)$$

Several interesting points can be noted concerning this expression. If we compare (18) to expression (1), which was used by Spear for the analysis of drift-mobility data,^{1,2} we see that Spear's formula is an approximation to ours. Although (1) and (18) are qualitatively similar, we see that (1) selects only one term from the summation in (18). The effect will be that Spear's formula underestimates μ_{ext} when used to fit experimental μ_d data; the second effect is that (1) will necessarily result in a well-defined activation energy of the drift mobility over most of the temperature range, where (18) would predict an activation energy which is temperature dependent. [Of course, if one term dominates the summation in (18), the result will be almost identical with Spear's formula.] Another observation concerns the status of (18). The reasoning which lead Spear to formula (1) was based on the assumption of quasiequilibrium and nondispersive transport.³¹ None of these assumptions were needed to arrive at (18), the only restriction being the validity of the detailed-balance result (12). [In the opposite case, one should use the full expression (13)]. Consequently, Spear's formula (1) has wider application than originally intended, but should be extended in the sense of (18).

Finally, it may be useful to recapitulate clearly the dependence of the transit time and drift mobility on the several parameters involved. First note that t_{tr} and μ_d are controlled only by those trap levels in which an electron falls at least twice during transit, as indicated by the prime in (13), (16), and (18). The other traps are defined to be deep traps. For a given DOS with given trap parameters $\sigma\bar{v}$ and a fixed μ_{ext} , it depends only on the sample parameter L/F (and *not* on the temperature, as one could intuitively assume) which traps are "deep" and which are "shallow" [see Eqs. (14) and (15)]. Note also that, according to this definition of deep traps, a level at 0.6 eV under E_c with a high density can act as a "shallow" trap, whereas a level with lower density at 0.3 eV can be "deep." Deep traps will only affect the amplitude and the shape of the transient photocurrent in a TOF experiment, but play a negligible role in the determination of t_{tr} and μ_d . We finally notice that the way in which the capture cross sections affect t_{tr} and μ_d is through the number of terms to be included in the primed summations. Indeed, as long as the detailed-balance result (12) is valid, the individual terms in these summations are not affected by an energy dependence of the cross sections, which is exactly balanced by the same energy dependence of ν . We therefore conclude that an analysis of drift-mobility data is not critically dependent on the value of the capture cross sections and the attempt-to-escape frequency, as long as the applied electric field F is not so high as to distort seriously the detailed-balance result (12). This circumstance is quite fortunate, as not much reliable information is available on these parameters.

We have now all the necessary formulas to analyze the drift mobility for a given model of the DOS and for given trap parameters. The transient photocurrent, which is proportional to the excess density of free carriers $n_c(t)$, can be obtained as the solution of the system of equations (4) and (5) in the pretransit time regime, and one obtains, in addition, the excess occupation of the traps $n_i(t)$. The transit time t_{tr} is obtained by forming a simple summation as in (16), from which follows the drift mobility

$$\mu_d = L/t_{tr}F. \quad (19)$$

Although the drift mobility defined by (19) is not necessarily an intensive material parameter (it will depend on F and L if transport is dispersive), it is the quantity obtained experimentally, and is therefore the appropriate one to consider in our simulations.

III. EXAMINATION OF THE TA AND ITS APPLICATION TO AN EXPONENTIAL DOS

Since the subjects of measured and calculated mobilities for α -Si:H and the thermalization approximation (TA) have to a certain extent become intertwined, it serves our purpose to start out by clearly defining what the TA consists of.^{15,16} If at $t=0$, n_0 excess carriers are injected into the transport states of a semiconductor, they rapidly will become trapped by the localized states, in proportion to the density and the capture cross section of these states. Trapped carriers are subsequently released into the transport states, but here the energy depth below the transport band at E_c comes into play. The average release time for carriers trapped in states at E_i is given by $\tau_{rel,i}$ in (6). Owing to the exponential dependence of $\tau_{rel,i}$ on the energy depth, carriers trapped in states at $E_i=0.8$ eV, for example, will in the average never reappear in the transport states on the time scale of an experiment (taking $\nu=10^{12}$ s⁻¹ and $kT=0.025$ eV, $\tau_{rel,i} \approx 10^{-2}$ s; this value is to be compared with a typical electron transit time of 10^{-7} s in α -Si:H). States at $E_i=0.1$ eV, on the other hand, will have released their trapped electrons many times during the same lapse of time (some 2000 times for the example at hand). It is therefore intuitively appealing to introduce a "demarcation energy" $E_d(t)$ defined by

$$E_d(t) = kT \ln(\nu t). \quad (20)$$

In the TA, one assumes that electrons below $E_d(t)$ remain frozen into the initial distribution, established roughly in a time $\tau_{trap} = W^{-1}$ [see Eq. (9)] after the flash excitation. Above $E_d(t)$, the electrons are "thermalized," which means that their density is related to the density of free carriers n_c by the appropriate Boltzmann factor.

According to (20), the demarcation level sinks with time into the distribution of localized states, thereby depopulating the states above E_d and adding more trapped charge to the states below E_d in addition to the already present frozen-in charge, such that the total density of excess carriers remains constant. Thus $E_d(t)$ acts in the way of a quasi-Fermi level,³² and the bulk of the injected charge will be concentrated near $E_d(t)$ in a decreasing DOS.

Whereas the TA is a general concept which in principle

is applicable to any DOS, practical use of it has been made almost exclusively for the case of an exponentially decreasing distribution of tail states (see, however, Ref. 5 and Sec. IV). This kind of analysis, introduced by Tiedje and Rose¹⁵ and Orenstein and Kastner¹⁶ is often referred to as TROK. In this work, we will indicate by TROK the TA applied to an exponentially decreasing DOS with a characteristic temperature T_c :

$$g(E) = g_0 \exp(-E/kT_c). \quad (21)$$

Tiedje *et al.*³ obtain an analytical expression for the fraction of free carriers (often designated as the θ factor):

$$n_c(t)/[n_c(t) + n_t(t)] = n_c(t)/n_0 = \frac{\alpha(1-\alpha)}{(\nu t)^{1-\alpha} - \alpha^2}, \quad (22)$$

where α is the “dispersion parameter” defined by

$$\alpha = T/T_c \quad (23)$$

and n_c and n_t are the densities of free and trapped excess charge, respectively, whereby $n_c + n_t = n_0$. It is seen from (22) that the pretransit current in a TOF experiment for this exponential DOS will decay approximately as a power law with power exponent $-(1-\alpha)$. This is in agreement with the Scher-Montroll theory of dispersive transport and with experimental results in, for example, α -As₂Se₃ (for a review, see Ref. 33).

After this brief overview of the ideas and results of the TA (for a more complete review, see Ref. 34) it should be pointed out that the application of these ideas to MT in an arbitrary DOS can lead to erroneous results as discussed by Marshall and Main¹⁷ and Marshall and Barclay.³⁰ These authors show that the TA analysis in terms of energy-dependent release probabilities, but ignoring variations of the DOS-determined capture probabilities, will only be applicable in specific instances (such as exponentially decreasing DOS).

Some of the initiators of the TA have proposed a more detailed analysis of multiple trapping.³⁵ However, rather than refining the approximations, they extend the domain of applications to more complex cases (energy-dependent cross sections, activated capture, etc.) while retaining the “orthodox” thermalization-depth concept. Whereas we certainly agree with these authors that such complicating features should probably be incorporated into the simple models, we feel that then there will be a need for refined analytical methods.

Let us therefore examine the application of the TROK model to the extended-state mobility of α -Si:H. We first compare the density of free carriers as obtained from the TROK analysis [formula (22)] with the result of our computational procedure. To this end, we discretize the DOS proposed by Tiedje *et al.*³ and shown in Fig. 2 (dashed) into 20 levels, equally spaced in the energy interval (0.0 eV, 0.30 eV). For the attempt-to-escape frequency ν , we chose the value deduced in Ref. 3 ($\nu = 4.6 \times 10^{11} \text{ s}^{-1}$); the trapping parameter $\sigma\bar{v}$ is then determined by the detailed-balance relation (12). The fact that this 20-level system is representative of the continuous distribution was checked by increasing the number of levels to 40, which did not change the results at all. As expected, the free-carrier

density $n_c(t)$ so obtained as the sum of 20 exponentials was indistinguishable from a power law with power exponent $-(1-\alpha)$, where α is the dispersion parameter defined in (23). (In fact, a smaller number of discrete levels can simulate approximate power-law behavior, as earlier demonstrated by Noolandi.²⁷) As far as the shape of $n_c(t)$ is concerned, the only difference between our result and (22) resides in the very-short-time behavior ($t \sim \nu^{-1}$) where our computation yields a better description of the initial trapping after the flash excitation, manifested in a deviation from the power law. We can also compare the absolute value of $n_c(t)$ with formula (22). Within a factor of 2, depending on the choice of ν , the agreement was very good. We may conclude from this that the TA, applied to an exponential DOS, gives reliable results for the density of free carriers, qualitatively as well as quantitatively. This conclusion is in agreement with the findings of Marshall and Barclay.³⁰

We next turn to the calculation of transit times and drift mobilities in TROK. As TROK was originally proposed to explain anomalously-dispersive transport, we first examine the TROK analysis for this transport mode; the question of the application of formulas derived for anomalously-dispersive transport to electron transport in α -Si:H—which is mildly dispersive at most—will be discussed later. Although the definition of a transit time in the case of highly dispersive transport is somewhat arbitrary (and is usually defined from the experimental point of view as the break point in a log-log plot of current versus time), one can agree to define t_{tr} as the time where the “center of gravity” of the free-excess charge reaches the back electrode of the sample. In the TROK analysis, this physical condition is identified with the formula³⁶

$$\int_0^{t_{tr}} \mu_{ext} F(n_c(t)/n_0) dt = L, \quad (24)$$

where F is the electric field and L the sample thickness.

Neglecting α^2 in (22) and substituting into (24), one obtains

$$t_{tr} = \nu^{-1} \left[\frac{\nu}{1-\alpha} \right]^{1/\alpha} \left[\frac{L}{\mu_{ext} F} \right]^{1/\alpha}. \quad (25)$$

This expression for the transit time can now be used to extract microscopic parameters from measured drift-mobility data. If the “time-dependent drift mobility” is defined as in Ref. 15 as

$$\mu_d(t) = \mu_{ext} n_c(t)/n_0, \quad (26)$$

one can use expression (22) to obtain

$$\mu_d(t) = \mu_{ext} \frac{\alpha(1-\alpha)}{(\nu t)^{1-\alpha} - \alpha^2}. \quad (27)$$

As the drift mobility is determined for $t = t_{tr}$, substitution of (25) into (27) will result in an expression which relates the microscopic parameters μ_{ext} and ν to the experimental quantities μ_d and α . This two-parameter curve-fitting procedure was used by Tiedje *et al.*³ in order to obtain ν and μ_{ext} for α -Si:H.

Under the assumption that an exponential distribution of localized states is an adequate DOS model for the ma-

material being studied, we now try to evaluate the errors introduced by this kind of analysis of μ_d data.

While it is true that in the case of *nondispersive* transport (24) simply states that $F\mu_d t_{tr} = L$, in agreement with the definition of drift mobility, we fail to see why this still should hold in the case of dispersive transport. In order to obtain an idea of the error introduced by the use of (25) for the calculation of transit times, we computed t_{tr} according to (16) after discretization of the exponential DOS (see Sec. II) and compared it to the result of (25). The DOS is given by (21), with $g_0 = 10^{21} \text{ cm}^{-3} \text{ eV}^{-1}$ (see Fig. 2, dashed line) and $T_c = 310 \text{ K}$. The trap and sample parameters, which will also be used in subsequent calculations, are summarized in Table I. Note that they are almost identical with the ones in Ref. 3. The choice of the sample thicknesses L_i in Table I was dictated by the fact that Tiedje *et al.*³ used a $3.9\text{-}\mu\text{m}$ thick sample at fields of 10^4 and $2 \times 10^4 \text{ V cm}^{-1}$. As it is L/F , rather than L/V (V the potential difference) which determines the transit time [see Eqs. (13) and (14)], our sample thicknesses L_2 and L_3 at the fixed field $F = 10^4 \text{ V cm}^{-1}$ are equivalent to Tiedje's experimental conditions. As already explained earlier, the choice of trapping parameter $\sigma\bar{v}$ determines the attempt-to-escape frequency ν through the detailed-balance condition (12) for each temperature used in the simulations. A few results are summarized in Table II and are compared to the result of (25), evaluated for the same system parameters. It is seen that the TROK analysis overestimates the transit time by a factor which depends on temperature. However, using $L/2$ of Ref. 15 instead of L of Refs. 3 and 34 in Eq. (25), one obtains values for the TROK transit time which are in fair agreement with the values from (16). The TROK analysis would then also imply a μ_{ext} value roughly twice as high as the one obtained by Tiedje *et al.*³

By still using formula (16), we are able to reconstruct μ_d versus $1/T$ curves for any given DOS, given only $\sigma\bar{v}$ and μ_{ext} . To test the interpretation of electron drift-mobility data in *a*-Si:H given by Tiedje *et al.*³ in terms of an exponential DOS, we performed such calculation, using the parameters in Table I. The results are shown in Fig. 3; the solid (open) circles are experimental points obtained by Tiedje *et al.* for a $3.9\text{-}\mu\text{m}$ sample at a field of 10^4 (2×10^4) V cm^{-1} and should be compared to curves L_3 and L_2 , respectively. It is seen that the good agreement between experimental and calculated drift mobilities of Ref. 3 is lost. Moreover, the simulations for the different sample thicknesses at a fixed field, which are equivalent to varying the field over one decade for sample

TABLE I. Trap and sample parameters used in the calculations of Secs. III, IV, and V.

Extended-state mobility	μ_{ext}	$10 \text{ cm}^2 \text{ V}^{-1} \text{ s}^{-1}$
Trapping parameters	$\sigma\bar{v}$	$10^{-15} \text{ cm}^2 \times 10^7 \text{ cm s}^{-1}$
Sample thickness	L_1	$1 \times 10^{-4} \text{ cm}$
	L_2	$1.95 \times 10^{-4} \text{ cm}$
	L_3	$3.9 \times 10^{-4} \text{ cm}$
	L_4	$10 \times 10^{-4} \text{ cm}$
Electric field strength	F	10^4 V cm^{-1}

TABLE II. Transit time according to Eq. (25) compared to the result of Eq. (16) for an exponential DOS as in Fig. 2 (dashed); other parameters as in Table I and $L = L_1 = 1 \mu\text{m}$.

Temperature (K)	t_{tr} (s)	t_{tr} (s)
	from (25)	from (16)
140	1.3×10^{-6}	3.0×10^{-7}
166	3.1×10^{-7}	8.8×10^{-8}
200	8.5×10^{-8}	2.6×10^{-8}
250	2.8×10^{-8}	9.8×10^{-9}
286	2.5×10^{-8}	6.2×10^{-9}

L_3 , show a rather strong dependence of the activation energy ΔE on temperature, sample thickness, and electric field. Although Tiedje's measurements do show some field dependence, the activation energy near room temperature is well defined and about 0.15 eV . This is in reasonable agreement with Spear,^{1,2} who found $\Delta E = (0.13 \pm 0.01) \text{ eV}$ for $150 < T < 300 \text{ K}$ and the electric field varying over one decade. In contrast, the simulation results of Fig. 3 show a strong field dependence, and in the experimental temperature range, a strong temperature dependence of μ_d . Moreover, the average activation energy for $222 < T < 286 \text{ K}$ is 0.11 eV for L_3 and 0.09 eV for L_2 (these two cases should correspond to the open and solid circles in Fig. 3), which is considerably lower than observed experimentally. To explain the field

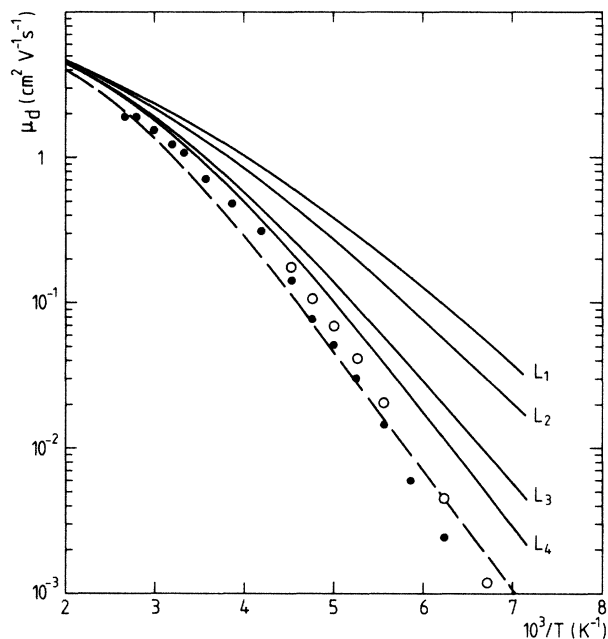


FIG. 3. Calculated drift mobilities for an exponential tail of localized states as considered by Tiedje *et al.* (Ref. 3) (dashed line in Fig. 1). The curves marked L_1 , L_2 , etc. correspond to the sample thicknesses given in Table I, where the other parameters used in the simulation are also summarized. The circles correspond to measured values. The open circles should be compared to curve L_2 , the solid circles to L_3 . The dashed curve was obtained with the use of the incorrect formula (29a).

and temperature dependence of ΔE at high temperature, Tiedje *et al.*³ invoke the *ad hoc* assumption of a “kinetic limit to thermalization.” In our view this discrepancy simply reflects the inadequacy of a pure exponential tail to describe the tail states in *a*-Si:H.

Further support for the consistency of our method is supplied by an alternative approach to calculate μ_d . To elaborate this alternative it will be useful to briefly discuss the drift-mobility concept, and try to elucidate some points which are not always clearly resolved in the literature. “Drift mobility” is not an unequivocal notion. Experimentally, it is determined according to (19) by measuring the transit time in a TOF experiment. As already remarked earlier, this drift mobility will be a meaningful (i.e., intensive) material parameter only when it is independent of L and F , at least in a reasonable interval. Loosely speaking, an intensive μ_d is equivalent to non-dispersive Gaussian transport, whereas a drift mobility which depends on L and F reflects anomalous dispersion. On the other hand, in most theoretical analyses of multiple-trapping transport, μ_d is mostly defined in the following manner. The expression is of the form

$$\mu_d = \mu_{\text{ext}} n_c / n_x, \quad (28)$$

where n_c is the excess free-carrier density. However, n_x is defined in several ways. There are essentially three versions:

$$\mu_d = \mu_{\text{ext}} n_c / n_0, \quad (29a)$$

with $n_0 = n_c + n_t$ the total injected excess charge;

$$\mu_d = \mu_{\text{ext}} n_c / n_t \quad (29b)$$

with n_t the trapped-excess charge; and

$$\mu_d = \mu_{\text{ext}} n_c / (n_t^* + n_c), \quad (29c)$$

where n_t^* is the density of trapped charge, *excluding excess charge in deep traps*. “Deep” traps should be understood in the sense explained in Sec. II. In amorphous semiconductors and at moderate temperatures, n_c is much smaller than n_t , such that forms (29a) and (29b) are practically equivalent in this case. It is one of these two versions which is used in analyses based on the TA.^{3,15,16} We think, however, that this is erroneous, at least in principle. The reason is understood by considering the transit-time formula (13) or (16). In the summation \sum' , only those traps are included which effectively control the transit time, i.e., which capture an electron at least twice (on average) during transit. In complete analogy, the expression for the drift mobility should include only the trapped electrons which are not in deep traps, and this gives (29c).

Our computational procedure of Sec. II allows us to calculate the drift mobility according to any of the above expressions. As the occupation of each trap species is known as a function of time, we simply have to add up the trapped electron density in the “shallow” states for (29c) (or more practically, to subtract the deep-trapped charge from n_0). Expression (29c) is then found to be only mildly time dependent and is practically a constant for t comparable to or larger than the transit time t_{tr} given by (16) (see also the next section). Performing such

calculations, we found that drift mobilities obtained from (18) (the curves shown in Fig. 3) are *exactly the same* as the results of the alternative approach (29c). This demonstrates the consistency of our method and the accuracy of the computations. On the other hand, a similar calculation, this time using (29a) (dashed curve in Fig. 3), gives agreement with curve L_3 only for the highest temperatures but comes closer to fitting the data than L_3 . The conclusion is as follows. In conjunction with expression (29a) and the DOS used by Tiedje *et al.*, our computational procedure gives results comparable to the ones from Tiedje’s analysis.³ In other words, in this instance, the use of the TA gives only minor differences with our presumably more accurate analysis. However, (29a) is incorrect and should be replaced by (29c) as argued above. When this is done, a more substantial discrepancy is seen between our simulations and Tiedje’s analysis. Although the TA could, in principle, give reliable results for DOS models analogous to the exponential tail considered here, it is not clear how (29c) could be incorporated into it.

We close this section with a short discussion of the evidence advanced by Tiedje in the case of *a*-Si:H in support of an exponential DOS, right up to the mobility edge, or at least for $0.08 < E < 0.30$ eV.³⁴ The TROK model implies a dispersion parameter α which is linear in temperature [see Eq. (23)]. However, the data in Ref. 3 deviate considerably from this behavior. Moreover, DOS models which differ considerably from the simple exponential tail have been shown³⁷ to give dispersion parameters which are difficult to distinguish from (23). Tiedje³⁴ also mentions the electron-spin resonance work of Dersch *et al.*³⁸ on doped *a*-Si:H as nontransport related evidence for the exponential DOS. Apart from the fact that the relation between spin density in doped material and the density of states in intrinsic material is not necessarily straightforward, we also observe that the approximate exponential increase in spin density found by Dersch *et al.* extends only up to ~ 0.3 eV below the conduction-band mobility edge. As the electron drift mobility is almost exclusively determined by states above this energy, this is hardly an argument in favor of the TROK interpretation. In our opinion, drift-mobility data rather point to the opposite conclusion: Our simulations show the simple exponential tail to be in contradiction with the almost field-independent drift-mobility activation energy observed experimentally.

IV. EXAMINATION OF THE DRIFT MOBILITY FOR SPEAR’S DOS

In this section we apply our computational procedure to the DOS model deduced by Spear¹ from field-effect measurements in *a*-Si:H. On the one hand, this will permit us to check the consistency of interpreting drift-mobility data obtained by Spear^{1,2} with this DOS; on the other hand, we will confront our results with Silver’s who estimated μ_{ext} to be about $500 \text{ cm}^2 \text{ V}^{-1} \text{ s}^{-1}$ on the basis of the TA and (29a) *referring to the same experimental data*.

To simplify the calculations, we have represented Spear’s DOS by a linear tail, followed by an exponential

$$g(E) = \begin{cases} g_0(\Delta - E)/\Delta, & 0 \equiv E_c \leq E \leq 0.12 \text{ eV} \\ g_a \exp\left[\frac{0.12 - E}{kT_c}\right], & 0.12 \leq E \leq 0.30 \text{ eV}, \end{cases} \quad (30a)$$

$$(30b)$$

where

$$g_0 = 5 \times 10^{20} \text{ cm}^{-3} \text{ eV}^{-1},$$

$$g_a = 4 \times 10^{19} \text{ cm}^{-3} \text{ eV}^{-1},$$

$$\Delta = 0.13 \text{ eV}, \quad T_c = 310 \text{ K}.$$

This model has an exponential tail with the same slope as in Tiedje's model,³ but is preceded by a linear part (see Fig. 2, solid line). It can be mentioned that the linear tail was not really a result of Spear's field-effect measurements, which gave the roughly exponential part only; rather, the linear tail was added to extend the DOS up to the conduction band, and the value of g_0 was a reasonable estimate. We are not concerned here with the reliability of field-effect measurements in relation to the bulk DOS; we simply check the consistency of the model with drift-mobility data. Needless to say that the analytical representation (30) of Spear's field-effect results is somewhat schematic; however, our simulations show that the calculated drift mobilities are not sensitive to small changes in the parameters of the DOS.

With the DOS given by (30) and parameters as in Table I, we performed calculations similar to the ones presented in Sec. III for the exponential DOS. The results are shown in Fig. 4 and can be compared to the experimental curve² (dashed in Fig. 4). Several points should be noted. Whereas Spear's measurements did not show any field dependence of the drift mobility¹ when the field was varied by a factor of 10, our simulations predict a rather large influence, as demonstrated by the distinct curves for the various sample thicknesses at a constant field (equivalent to a field variation by a factor of 10 for fixed sample thickness, as explained in Sec. III). We also find a drift-mobility activation energy ΔE which depends on the temperature and the field. For sample L_3 , ΔE is 0.148 eV for the higher temperature range ($222 < T < 286$ K) and increases to 0.168 eV for the lower temperatures ($154 < T < 222$ K). There is also a misfit between the calculated and experimental curves with respect to the absolute values. For L_3 , e.g., the factor ranges from 5 to 10. To a good approximation, the calculated curves can be shifted vertically by multiplying μ_{ext} by such factor [see Eq. (18); note, however, that μ_d depends on μ_{ext} not only by a factor, but also through the number of terms to be included in the summation, see Eq. (15)]. As the value $\mu_{\text{ext}} = 10 \text{ cm}^2 \text{ V}^{-1} \text{ s}^{-1}$ was chosen in our simulations (see Table I), this means that the experimental data would imply an extended-state mobility of about $50 \text{ cm}^2 \text{ V}^{-1} \text{ s}^{-1}$ if the DOS were correct. This conclusion is not altered when we take a capture cross section which is 10 times larger than in Table I, resulting in $\sigma\bar{v} = 10^{-7} \text{ cm}^3 \text{ s}^{-1}$. The result of such calculation is shown in Fig. 5. The curves have a better resemblance to the experimental data

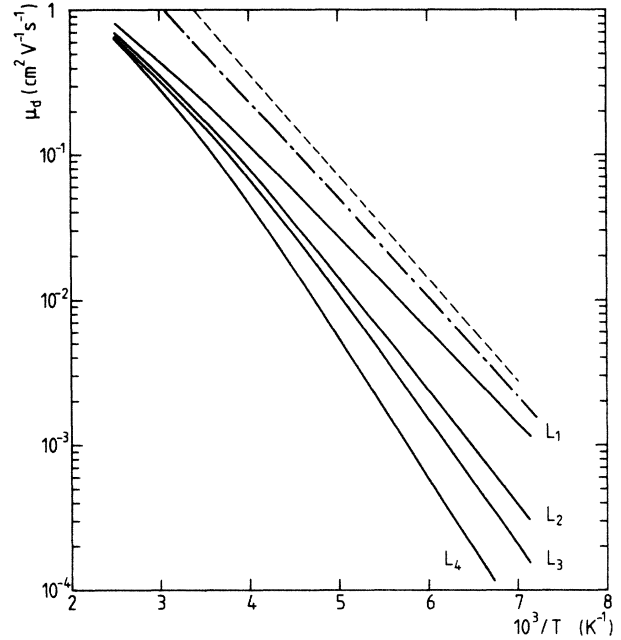


FIG. 4. Calculated drift mobilities for the distribution of tail states proposed by Spear (Ref. 1) on the basis of field-effect measurements (solid line in Fig. 1). The curves marked L_1 , L_2 , etc. correspond to the sample thicknesses given in Table I, where the other parameters used in the simulation are also summarized. The dashed curve represents Spear's experimental results. The dashed-dotted line is based on formula (1), which was used by Spear for analysis of these data.

in that the drift-mobility activation energy is less field dependent, but a fit to the experimental data would now imply an even larger value for the extended-state mobility ($\sim 70 \text{ cm}^2 \text{ V}^{-1} \text{ s}^{-1}$).

The reason for the discrepancy between our analysis and Spear's can be traced back to the use of (1), which is an approximation to formula (18) used in our calculations. In Fig. 4, we have also plotted the result of formula (1) with the same parameters substituted as in our simulations (dashed-dotted line). It is clear that only slight changes in the parameters are needed to obtain a perfect fit with the experimental data; however, we think that a good fit is not sufficient to obtain reliable results. If Spear's DOS could be properly represented by one dominant level, as implicitly assumed in formula (1), the inclusion of other levels representing Spear's DOS should not affect the results. In this case, (1) and (18) should be equivalent. However, our simulations show that this is not the case, and the reduction of Spear's DOS to a single level is unwarranted.

The second issue to be discussed in this section is the result of Silver, Snow, and Adler,⁵ who deduced $\mu_{\text{ext}} \approx 500 \text{ cm}^2 \text{ V}^{-1} \text{ s}^{-1}$ referring also to Spear's experimental data. When we apply our procedure to the DOS models considered in Ref. 5, we find μ_{ext} values which are in good agreement with that of Silver *et al.*, including values of several thousand $\text{cm}^2 \text{ V}^{-1} \text{ s}^{-1}$ for some particular models.

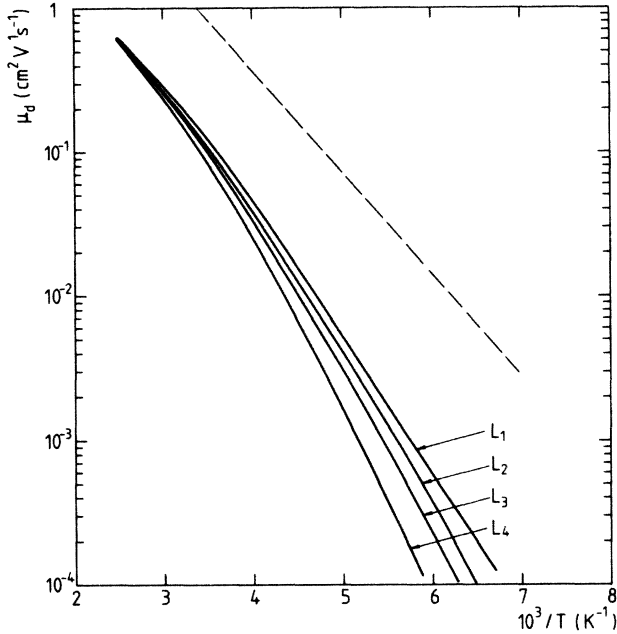


FIG. 5. Calculated drift mobilities for the distribution of tail states proposed by Spear; the parameters used and the meaning of the symbols are the same as in Fig. 4, except that the capture cross sections here are 10 times larger than for Fig. 4. The dashed curve represents Spear's experimental results.

Conversely, applying the analysis outlined in Ref. 5 to the DOS considered previously in this section [Eq. (30)], we again find only minor differences with our results. This shows once again that the TA can be successfully applied to a certain class of DOS models. However, our simulations show that none of the models considered by Silver *et al.* in Ref. 5 are compatible with the experimental data. We considered, e.g., case B of Ref. 5 with $E_0 = 0.14$ eV; this consists of an exponential tail with $T_c = 812$ K for $E_c < E < E_0$ and a steeper exponential with $T'_c = 313$ K for $E > E_0$. The other parameters were taken from Ref. 5: $\mu_0 = 480$ cm² V⁻¹ s⁻¹, $\sigma\bar{v} = 4.6 \times 10^{-8}$ cm³ s⁻¹, the latter value resulting from the detailed-balance relation (12), and $\nu = 10^{12}$ s⁻¹ as in Ref. 5. We performed the simulations for a 5- μ m thick sample and for electric field ranging from 10^3 V cm⁻¹ to 5×10^4 V cm⁻¹. We then find that the drift mobility at room temperature is about 4, rather than 1 cm² V⁻¹ s⁻¹ as in Ref. 5. Also, there is a considerable field dependence (dispersion) of μ_d , and the drift-mobility activation energy varies from 0.23 eV for the lowest field to 0.17 eV for the highest, in sharp contrast with experiment.

One reason why this deficiency in the DOS models considered by Silver *et al.*⁵ was not observed lies in their use of *experimentally* determined values for the transit time t_{tr} , for which values

$$\mu_{ext} = \mu_d(t_{tr})n_i(t_{tr})/n_c(t_{tr})$$

are evaluated. In our approach, on the other hand, t_{tr} is calculated according to the model parameters with Eq.

(16), and this allows us to make a thorough comparison between model predictions and experimental data.

Another feature which could be checked by our simulation procedure is the shape of the pretransit current. Figure 6 shows calculated pretransit current traces for Spear's DOS. It is seen that approximate power-law behavior for $t \sim t_{tr}$ is not restricted to the pure exponential tail. For this nonexponential DOS, one can define quite easily the "dispersion parameter" α (1 plus the slope of the current in a log-log plot) which is shown in the inset of Fig. 6. The α curve agrees rather well with expression (23) which was derived for a pure exponential tail.

V. INVESTIGATION OF OTHER DOS MODELS

As we have seen in the two preceding sections, neither of the two DOS models investigated—the exponential DOS proposed by Tiedje *et al.*³ or the "hybrid" linear-exponential distribution based on the field-effect measurements by Spear¹—gives good agreement with the drift-mobility data. However, it seems likely that there is no universal DOS for *a*-Si:H, irrespective of the origin and preparation conditions of the material. Whereas Tiedje's drift-mobility data exhibit a certain field dependence when the field is altered by only a factor of 2, Spear's data show no such dependence even for a field variation over one decade. (Incidental as it may be, Spear's DOS seems to give a better fit to Tiedje's data, at least qualitatively.) One feature we further investigated is the discrepancy between Spear's μ_d data and the DOS deduced from his

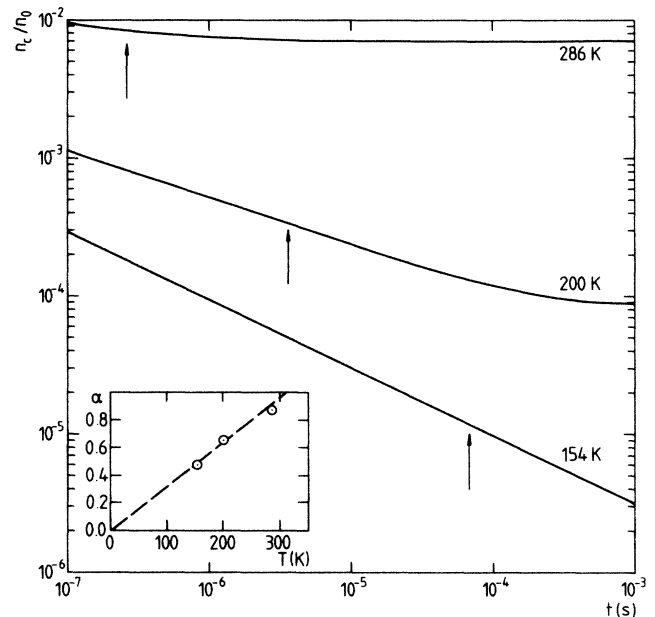


FIG. 6. Occupation of the conduction band by excess carriers at several temperatures, calculated for Spear's DOS. The curves have the same shape as the pretransit-time photocurrent would have for this distribution. The arrows indicate the transit time for sample L_3 under a field $F = 10^4$ V cm⁻¹. The inset shows the dispersion parameter α for the three curves, and is compared to the curve $\alpha(T) = T/T_c$ with $T_c = 310$ K (dashed).

field-effect measurements. As shown in Sec. IV, the main problem is the degree of dispersion, which is absent in the experimental data, but rather high according to our simulations, as reflected by the distinct curves obtained for different sample thicknesses at a constant field (see Figs. 4 and 5). There are several possibilities to remedy this discrepancy. If, for instance, there were a pronounced peak in the DOS at a depth of about 0.14 eV below the conduction band, this would pin the drift-mobility activation energy at about this energy and make it independent of the applied field, the more so the higher the peak. With such a peak, Spear's analysis based on formula (1) would be well suited and we anticipate that our analysis based on (18) would come in closer agreement with (1). We have examined such peaked distribution by adding a pronounced trapping level with a width of 0.015 eV at $E = 0.135$ eV in the DOS model (30). Even when this level protrudes by only a factor of 3 above the normal background (this corresponds to the rectangle in Fig. 2), the activation energy ΔE changes by less than 0.01 eV for moderate temperatures on changing the field by a factor of 10. This is shown in Fig. 7. We find $\Delta E \approx 0.14$ eV, in agreement with Spear's data. [Note, however, that one would deduce $\mu_{\text{ext}} \approx 100 \text{ cm}^2 \text{ V}^{-1} \text{ s}^{-1}$ on the basis of Fig. 7 and in agreement with formula (1).] We also found that the transient photocurrent in this case differs very little from the case without the added feature, at least on an experimental time scale. Higher peaks make ΔE virtually independent of the field even at the lowest temperatures, but are betrayed by the shape of the current. In agreement with other work,³⁹⁻⁴¹ we find that the peak should protrude by about a factor of 5 above the local back-

ground in order to be observable in a TOF experiment.

Another possibility which we investigated is that the DOS used in Sec. V and analytically represented by (30) is only one of the several models which are compatible with Spear's field-effect measurements. In a recent publication,² Hourd and Spear found that the drift-mobility data are better fitted when the ratio g_0/g_a [see Eq. (30)] is about 30, rather than 12 as in Sec. IV. We therefore replaced the linear tail (30a) by a steeper one, with $g_0 = 10^{21} \text{ cm}^{-3} \text{ eV}^{-1}$, all other parameters being kept as before (dotted line in Fig. 2). This gives a ratio $g_0/g_a = 25$. The results are shown in Fig. 8. Shifting the curves vertically so as to make $\mu_d = 1 \text{ cm}^2 \text{ V}^{-1} \text{ s}^{-1}$ at room temperature would now result in an extended-state mobility of about $30 \text{ cm}^2 \text{ V}^{-1} \text{ s}^{-1}$. However, the curves exhibit the same dispersion as before and we conclude that this version of Spear's DOS gives no better agreement with the experimental drift-mobility data.

A third possibility has been suggested by Marshall^{2,19} and consists in a change in the nature of the localized states as one passes beyond $E \approx 0.13$ eV from the tail states into the gap states. If states below this energy possessed an appreciably smaller cross section for electrons than those above, they would have little effect on the propagation of the excess carriers in a TOF experiment. Our simulations corroborate this hypothesis. For the DOS, we took (30) with the same parameters as for Fig. 4, i.e., $\bar{v} = 10^7 \text{ cm s}^{-1}$, $\sigma = 10^{-15} \text{ cm}^2$; however, for the states below 0.135 eV the capture cross section was set equal to 10^{-16} cm^2 . The result is shown in Fig. 9. The four curves now coalesce into one, reflecting the nondispersive

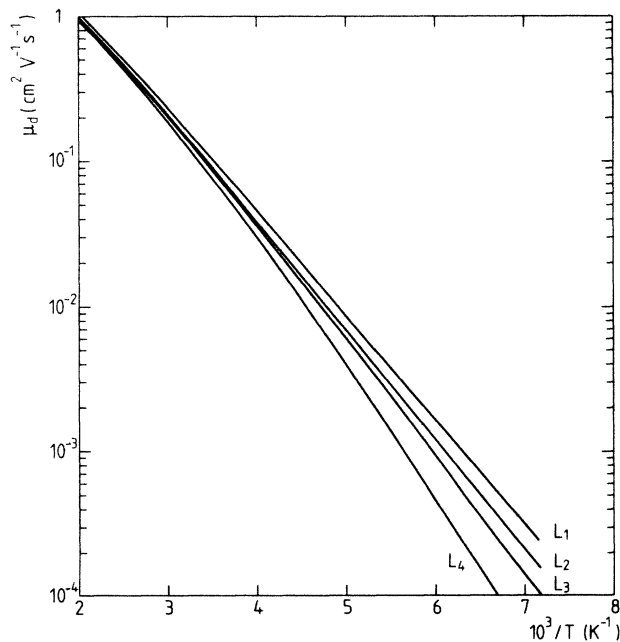


FIG. 7. Calculated drift mobilities for the distribution of tail states proposed by Spear (Ref. 1) but with a peak added at $E = 0.135$ eV below the conduction band (shown as the dashed line in Fig. 2). The system parameters used and the meaning of the symbols are the same as used in Fig. 4.

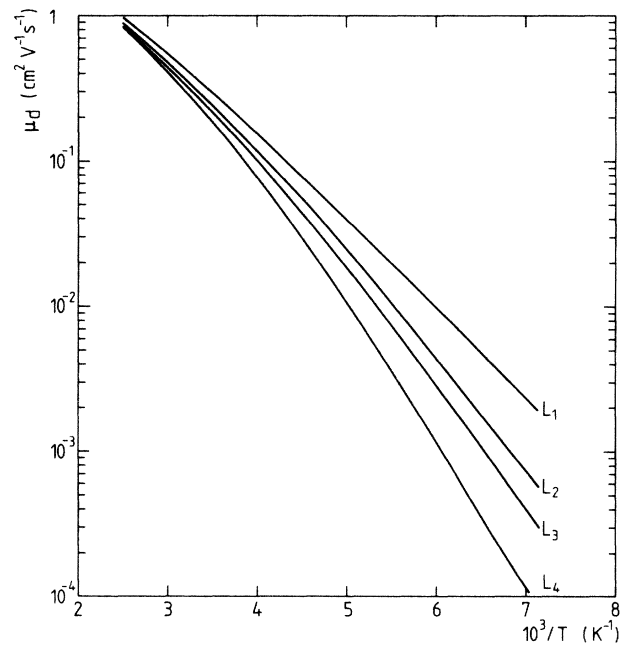


FIG. 8. Calculated drift mobilities for a variation of Spear's DOS, proposed by Hourd and Spear (Ref. 2). This distribution has the same exponential tail as used for Figs. 4 and 5, but the linear part starts from $g(E) = 10^{21} \text{ cm}^{-3} \text{ eV}^{-1}$ instead of $5 \times 10^{20} \text{ cm}^{-3} \text{ eV}^{-1}$. The other system parameters used and the meaning of the symbols are the same as in Fig. 4.

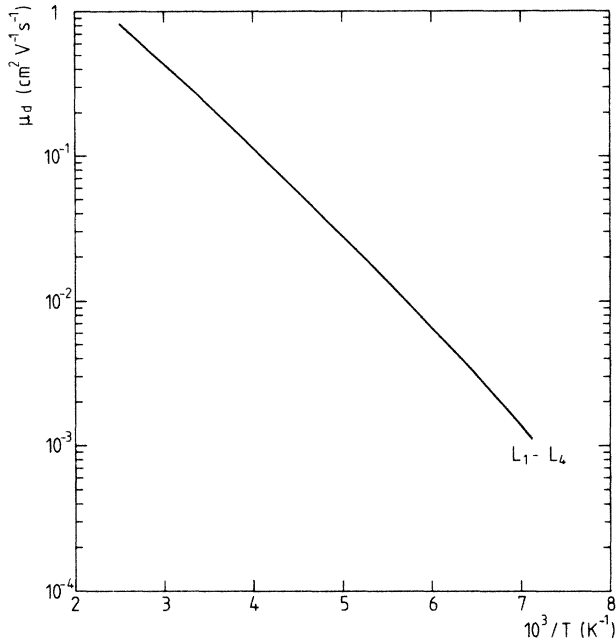


FIG. 9. Calculated drift mobilities for a variation of Spear's DOS, proposed by Marshall (Ref. 19). This distribution is identical to the one used for Figs. 4 and 5 (solid line in Fig. 1) but the capture cross sections drop abruptly from the value 10^{-15} cm^2 to 10^{-16} cm^2 when passing the energy 0.135 eV. The other system parameters used and the meaning of the symbols are the same as in Fig. 4. Curves L_1-L_4 now coalesce into one.

nature of the transport over the entire temperature range that is considered. The drift-mobility activation energy is about 0.12 eV. It is clear that one could obtain almost perfect agreement with Spear's experimental mobility data by slight changes in the parameters. The deduced extended-state mobility would be about $30 \text{ cm}^2 \text{ V}^{-1} \text{ s}^{-1}$. The "good fit" obtained above should not be considered as direct evidence for the localized state distribution and the parameters used in the simulation. A closer look at the computations reveals that the introduction of a sharp drop in the capture cross sections for the gap states simply eliminates any role played by the exponential part of the DOS with respect to the calculation of the transit time and the drift mobility. The reason why the four curves coalesce in Fig. 9 is that exactly the same traps (those in the linear part of the distribution) are included in the primed summations (13), (16), and (18), irrespective of the sample thickness. Speaking in more physical terms, the same set of traps is visited at least twice (on the average) and thus controls the transit time. Exactly the same result would be obtained if we considered a DOS with a linear distribution of tail states and a sharp cutoff below, because it is always the density multiplied by $\sigma\bar{v}$ which determines the trapping kinetics. This does not imply that both models would be equivalent in all respects. The presence of deep traps, which are inert as far as the determination of t_{tr} and μ_d is concerned, betray themselves in the shape of the transient excess current. This is illustrat-

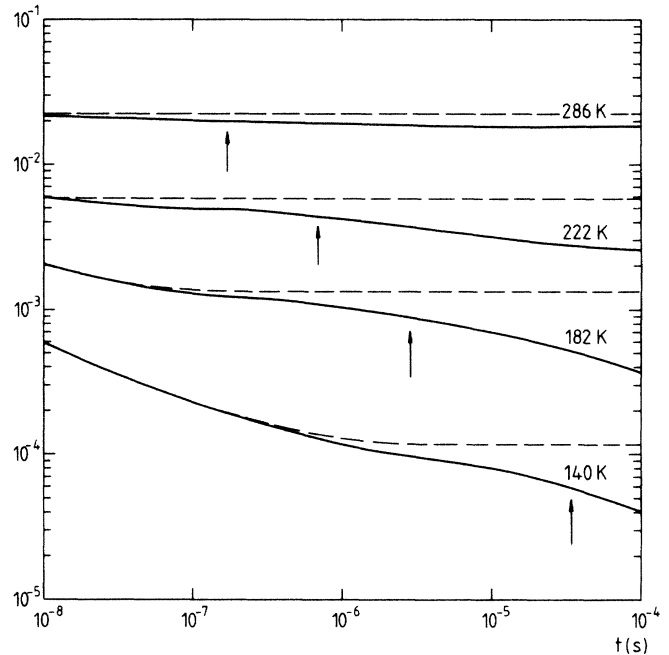


FIG. 10. Occupation of the conduction band by excess carriers at several temperatures, calculated for the variation of Spear's DOS proposed by Marshall (Ref. 19) and which exhibits a sharp drop in the capture cross sections for states below 0.135 eV (solid lines). The transient photocurrent would show the same shape for times comparable to the transit time (indicated by arrows and corresponding to sample L_3). If the states with the smaller capture cross sections are eliminated from the distribution, featureless current traces result, shown as dashed lines in the figure.

ed in Fig. 10. The solid curves give the occupation of the conduction band at several temperatures for the DOS considered in Fig. 9, i.e., the distribution (30) with a sharp drop in the capture cross sections for states deeper than 0.135 eV under the conduction band. One sees that the transient photocurrent would exhibit structure for times comparable to the transit time (indicated by arrows in Fig. 10). On the other hand, if we simply cut off the states below 0.135 eV, almost featureless current traces would result (dashed in Fig. 10) even at the lowest temperatures. As the experimental TOF currents in $a\text{-Si:H}$ do show a power-law behavior at low temperatures for $t \leq t_{tr}$ rather than a plateau, one could speculate that a drop in the capture cross sections as proposed by Marshall is a real feature. However, a linear tail of shallow states and some distribution of deep gap states would have an analogous effect. We cannot decide on the basis of the present experimental evidence which model is best suited to explain the whole realm of phenomena in $a\text{-Si:H}$.

VI. CONCLUSIONS

In this study, we have introduced a novel method of analyzing transient photocurrents and drift-mobility data in amorphous semiconductors, and as a first application

we have examined the controversy surrounding the interpretation of experimental electron drift mobilities in *a*-Si:H. Our general method is based on the discretization of a continuous distribution of localized states, and results in a simple and accurate computational procedure which allows the study of trap-controlled band transport ("multiple trapping") in an arbitrary DOS. Although drift-mobility data alone are not sufficient to deduce unequivocally the distribution of the tail states, it has been demonstrated that a simulation-assisted analysis of such data can eliminate one class of models and favor another one. In this respect, drift-mobility measurements over a large temperature interval give an almost unique opportunity to obtain information on the distribution of the tail states in the vicinity of the mobility edge, since other experimental methods such as field effect, space-charge-limited currents, or transient photocurrent spectroscopy are very insensitive to these states.

With respect to the interpretation of electron drift-mobility data in *a*-Si:H, we have reached several conclusions. In the first place, the tail-state distribution (at least for the conduction band) seems to be different for material obtained in different laboratories, as reflected by the different degree of dispersion in Tiedje's data³ as compared to Spear's.^{1,2} A second conclusion is that additional features are needed in order to reconcile the DOS model proposed by Spear on the basis of field-effect measurements¹ with the nondispersive drift mobility. Such features could be a sharp drop in the DOS or the capture cross sections for states below $E \approx 0.14$ eV, or a peak

around that energy. It is interesting to note that the unaltered Spear model is qualitatively in better agreement with Tiedje's data, which do exhibit a certain degree of dispersion at the lower temperatures.

We also found that the best fit to Spear's experimental data was obtained with a somewhat higher extended-state mobility ($\mu_{\text{ext}} \approx 50 \text{ cm}^2 \text{ V}^{-1} \text{ s}^{-1}$) than presumed before. However, we also find that no realistic choice of the parameters used in the simulations would result in the quasi-crystalline value $\mu_{\text{ext}} = 500 \text{ cm}^2 \text{ V}^{-1} \text{ s}^{-1}$ deduced by Silver⁵ to fit the same experimental data that are the object of our simulation.

Finally, apart from the conclusions reached for the case of *a*-Si:H, we have also discussed some features which apply to the analysis of TOF experiments in the general case of an amorphous semiconductor with a structured DOS in the gap. Whereas we found only minor differences between the results of our analysis and the TA when applied to a monotonously decreasing DOS, more substantial differences would arise in the general case (see, e.g., Ref. 41). It then becomes important to distinguish properly between shallow and deep trapping, as discussed with respect to formula (29).

ACKNOWLEDGMENTS

This work was supported in part by the Belgian Interuniversitair Instituut voor Kernwetenschappen. One of us (G.A.) would like to thank M. Silver for valuable comments on various aspects of this work.

¹W. E. Spear, *J. Non-Cryst. Solids* **59-60**, 1 (1983).

²A. C. Hourd and W. E. Spear, *Philos. Mag.* **B 51**, L13 (1985).

³T. Tiedje, J. Cebulka, D. Morel, and B. Abeles, *Phys. Rev. Lett.* **46**, 1425 (1981).

⁴N. F. Mott, *Philos. Mag.* **B 51**, 19 (1985).

⁵M. Silver, E. Snow, and D. Adler, *Solid State Commun.* **51**, 581 (1984).

⁶N. F. Mott and E. A. Davis, *Electronic Processes in Non-Crystalline Materials*, 2nd ed. (Clarendon, Oxford, 1979), p. 219.

⁷M. Silver, E. Snow, M. Aiga, V. Cannella, R. Ross, Z. Yaniv, M. Shaw, and D. Adler, *J. Non-Cryst. Solids* **59-60**, 445 (1983).

⁸J. Tauc, in *Semiconductors and Semimetals*, edited by J. Panikove (Academic, New York, 1984), Vol. 21B.

⁹M. Silver and D. Adler, *Optical Effects in Amorphous Semiconductors*, Proceedings of the International Topical Conference on Optical Effects in Amorphous Semiconductors (Snowbird, Utah, 1984), AIP Conf. Proc. No. 120, edited by P. C. Taylor and S. G. Bishop (AIP, New York, 1984), p. 197.

¹⁰M. Silver, E. Snow, and D. Adler, *Solid State Commun.* **54**, 15 (1985).

¹¹M. Silver, E. Snow, N. C. Giles, M. P. Shaw, V. Cannella, S. Payson, R. Ross, and S. Hudgens, *Physica* **117& 118B**, 905 (1983).

¹²M. Silver, E. Snow, B. Wright, M. Aiga, L. Moore, V. Cannella, R. Ross, S. Payson, M. P. Shaw, and D. Adler, *Philos. Mag.* **B 47**, L39 (1983).

¹³W. E. Spear and H. Steemers, *Philos. Mag.* **B 47**, L77 (1983).

¹⁴H. Steemers, W. E. Spear, and P. G. LeComber, *Philos. Mag.* **B 47**, L83 (1983).

¹⁵T. Tiedje and A. Rose, *Solid State Commun.* **37**, 49 (1981).

¹⁶J. Orenstein and M. Kastner, *Phys. Rev. Lett.* **46**, 1421 (1981).

¹⁷J. M. Marshall and C. Main, *Philos. Mag.* **B 47**, 471 (1983).

¹⁸H. Michiel, J. M. Marshall, and G. J. Adriaenssens, *Philos. Mag.* **B 48**, 187 (1983).

¹⁹J. M. Marshall, P. G. LeComber, and W. E. Spear, *Solid State Commun.* **54**, 11 (1985).

²⁰It would be more correct to use the density of *unoccupied* states $g(E)[1-f(E)]$ in Eq. (2), with $f(E)$ the Fermi function. However, since states near the Fermi level play a negligible role in MT transport for wide-band-gap materials as *a*-Si:H, we neglect the occupation statistics. If so desired, they can be easily incorporated into the calculations.

²¹We call \bar{v} an average velocity, rather than the thermal velocity since, according to N. F. Mott, the velocity of electrons at the band edge is not thermal, but is given by $\sim \hbar/ma$, where m is the electron mass and a the scattering length. See R. A. Street, *Appl. Phys. Lett.* **41**, 1060 (1982). Both approaches give approximately the same value $\bar{v} = 10^7 \text{ cm s}^{-1}$. One could also question the validity of the use of a capture cross section to describe the capture process. If desired, one could use a general trapping rate constant $b(E)$ instead of $\sigma(E)\bar{v}$, but this does not affect our analysis. The use of a capture cross section is linked to the assumption of ballistic (rather than diffusive) transport; which of those relates to interaction with

- the traps relevant to the drift mobility is not evident.
- ²²V. Halpern, *Philos. Mag.* B **49**, L57 (1984).
- ²³A. I. Rudenko and V. I. Arkhipov, *Philos. Mag.* B **45**, 177 (1982).
- ²⁴V. I. Rudenko and A. I. Arkhipov, *Philos. Mag.* B **45**, 189 (1982).
- ²⁵H. Michiel and G. J. Adriaenssens, *Philos. Mag.* B **51**, 27 (1985).
- ²⁶The use of the more correct expression $N_i = \int_{E_i - \delta E/2}^{E_i + \delta E/2} g(E) dE$ has negligible influence for small δE as used in our simulations.
- ²⁷F. W. Schmidlin, *Phys. Rev. B* **16**, 2362 (1977); J. Noolandi, *ibid.* **16**, 4466 (1977).
- ²⁸K. Maschke, E. Merk, and W. Czaja, *Helv. Phys. Acta* **58**, 517 (1985).
- ²⁹S. W. Ing, J. H. Neyhart, and F. Schmidlin, *J. Appl. Phys.* **42**, 696 (1971).
- ³⁰J. M. Marshall, *J. Non-Cryst. Solids* **77-78**, 425 (1985); J. M. Marshall and R. P. Barclay, in *Physics of Disordered Materials*, edited by D. Adler, H. Fritzsche, and S. R. Ovshinsky (Plenum, New York, 1985), p. 567.
- ³¹In this article, as elsewhere in the literature, the terms “non-dispersive,” “conventionally dispersive,” or “Gaussian” are used interchangeably; “dispersive” should be understood as “anomalously dispersive” or “non-Gaussian.”
- ³²E. A. Schiff, *Phys. Rev. B* **24**, 6189 (1981).
- ³³G. Pfister and H. Scher, *Adv. Phys.* **27**, 747 (1978).
- ³⁴T. Tiedje, in *Semiconductors and Semimetals*, edited by J. Pankove (Academic, New York, 1984), Vol. 21C, p. 207, and in *The Physics of Hydrogenated Amorphous Silicon*, edited by J. D. Joannopoulos and G. Lucovsky (Springer-Verlag, New York, 1984), Vol. 2, p. 261.
- ³⁵D. Monroe and M. A. Kastner, *Philos. Mag.* B **47**, 605 (1983).
- ³⁶In Ref. 15, $L/2$ is used as the rhs of (26) rather than L . This explains the difference between formula (1) of Ref. 3 and formula (10) of Ref. 15.
- ³⁷J. M. Marshall, H. Michiel, and G. J. Adriaenssens, *Philos. Mag.* B **47**, 211 (1983).
- ³⁸H. Dersch, J. Stuke, and J. Bleicher, *Phys. Status Solidi B* **105**, 265 (1981).
- ³⁹J. M. Marshall and R. Street, *Solid State Commun.* **50**, 91 (1984).
- ⁴⁰M. Silver, E. Snow, and D. Adler, *Solid State Commun.* **53**, 637 (1985).
- ⁴¹G. Seynhaeve, G. J. Adriaenssens, and H. Michiel, *Solid State Commun.* **56**, 323 (1985).